International Forum on Aeroelasticity and Structural Dynamics
IFASD 2017
25-28 June 2017, Como - Italy

COMPARISON OF DIFFERENT APPROACHES FOR MODELING OF ATMOSPHERIC EFFECTS LIKE GUSTS AND WAKE-VORTICES IN THE CFD CODE TAU

R. Heinrich and L. Reimer

DLR Institute of Aerodynamics and Flow Technology
Lilienthalplatz 7
38108 Braunschweig
ralf.heinrich@dlr.de, lars.reimer@dlr.de

Keywords: Gust encounter, wake vortex encounter, disturbance velocity approach, resolved atmosphere approach, unsteady simulation.

Abstract: Two different methods for modeling of atmospheric effects have been implemented into the CFD code TAU. The first one is the so called disturbance velocity approach, a simplified method which allows predicting the influence of gusts or wake vortices on the aircraft, but not vice versa. Alternatively, an unsteady boundary condition has been implemented to feed in the atmospheric disturbances into the flow field. Thereby the mutual interaction of atmospheric disturbances and aircraft is captured. Both methods are compared for 3D applications in order to access the validity range of the simplified approach. A result is that the simplified approach is sufficient accurate for scenarios relevant for the certification process of aircraft. Even for a gust wavelength down to one reference chord length the agreement of the highly accurate method and simplified approach is fair. To demonstrate the capability of the simplified method for industrial applications, the maneuver of a generic fighter configuration through the wake vortices of an aircraft in front is simulated. The reaction of the aircraft due to the additional loads has been taken into account by coupling of CFD with flight mechanics.

1 INTRODUCTION

The prediction of unsteady loads caused by atmospheric effects like gusts and wake vortices is essential for aircraft development. The knowledge of the additional loads arising is of importance for the design of the structure but also for the layout of the control surfaces and the flight control system. To predict these additional air loads two different approaches for modeling of atmospheric disturbances have been implemented in the CFD code TAU [1].
One of these methods is the so called Disturbance Velocity Approach (DVA) [2]. In literature this method is also known as Field Velocity Approach (FVA) [3]. This method is straight forward to implement in CFD codes and allows the usage of standard meshes, which usually are characterized by a reduced mesh resolution with growing distance from the aircraft. The method captures the influence of e.g. a gust on the aircraft, but is not able to predict the feedback of the aerodynamics of the aircraft on the gust shape. Therefore, especially for gusts of short wavelength, a prediction error can be expected. To get a clearer view of the range of validity of the DVA an alternative method has been implemented in TAU: The atmospheric disturbances can be fed into the discretized flow field using an un-steady boundary condition at the far field boundaries. The advantage of the method is that the mutual interaction of the atmospheric disturbances and aircraft is captured, since they are resolved in the flow field.

Therefore the abbreviation of this approach is RAA in the following standing for Resolved Atmosphere Approach. However, a high resolution in the whole domain is required, to transport the disturbances from the inflow boundary to the aircraft without too much numerical losses.
In the following the DVA and RAA are described at first and, afterwards, both methods are compared for gust and wake vortex encounter scenarios. The strategy to simulate the mutual interaction using the unsteady boundary condition is described in detail. To demonstrate the capability of the DVA for industrial applications, the wake vortex encounter of a generic fighter aircraft with the wake vortices of a larger aircraft in front is presented in chapter 3. In this simulation the reaction of the aircraft due to the additional loads is captured by coupling of aerodynamics and flight mechanics.

2 MODELING OF ATMOSPHERIC EFFECTS IN TAU

2.1 Disturbance Velocity Approach

To enable the simulation of an aircraft interacting with atmospheric effects, several approaches are possible. One popular method is the DVA, which has been implemented into the block structured DLR FLOWer code [4] for the simulation of the influence of wake-vortices of a large leading aircraft model on the loads of a smaller aircraft model following [2]. Good agreement to experimental data was found for steady simulation. Motivated by the success of this method, the DVA has now also been implemented into the hybrid TAU-code.
In this method the flux balance is slightly altered by superposition of an additional disturbance velocity field $\mathbf{v}_i$ induced by e.g. a gust. $\mathbf{v}_i$ is prescribed as a function of space and time, depending on the shape and position of the gust. The convection across the cell interface of a control volume changes from $\mathbf{v} - \mathbf{v}_b$ to $\mathbf{v} - \mathbf{v}_b - \mathbf{v}_i$ with $\mathbf{v}_b$ being the velocity of the boundary of a control volume. For example the continuity equation then changes to

$$\frac{d}{dt}\int_V \rho dV + \oint_S \rho(\mathbf{v} - \mathbf{v}_b - \mathbf{v}_i)dV = 0 \quad . \tag{1}$$

Figure 1 shows a gust with wavelength λ_{gust} and amplitude v_{gust} moving with a speed of u_{inf} relative to an airfoil. The shape of the gust is specified as a function of the coordinate x and time t. In the upper part of Figure 1 ($t = t_1 = 0$), the distribution of disturbance velocity normalized with the amplitude of the gust is shown, if the gust is in front of the airfoil. In the lower part of Figure 1 the gust is just beneath the airfoil ($t = t_2$) and again the disturbance velocity field is shown, which moved a distance of $\Delta x = (t_2 - t_1)\, u_{inf}$,. The local effect of the gust is approximately the same, as if the airfoil is moving with the negative gust vertical speed $\mathbf{v}_i\,(x,t)$ downward. More about the motivation and verification of this method may be found in [5].
In TAU it is possible to prescribe atmospheric disturbances using analytical functions. Alternatively an arbitrary disturbance velocity field can be prescribed on an equidistant Cartesian auxiliary mesh. In dependency of the actual position of the aircraft the disturbance velocity field is interpolated from the Cartesian mesh to all nodes of the aircraft mesh, if the DVA is used. For the RAA the interpolation is restricted to the far field boundaries.
For gust encounter simulations gusts with a “1-cos” shape as described in the Federal Aviation Regulations (FAR) part 25.341 can be defined. The amplitude of the gust v_{gust} and the wavelength λ_{gust} are input parameters. Vertical as well as lateral gusts can be specified. The user can select between isolated gusts and sequences of gusts. The extension of the gusts in spanwise direction (vertical gusts) and vertical direction (lateral gusts) can also be specified.

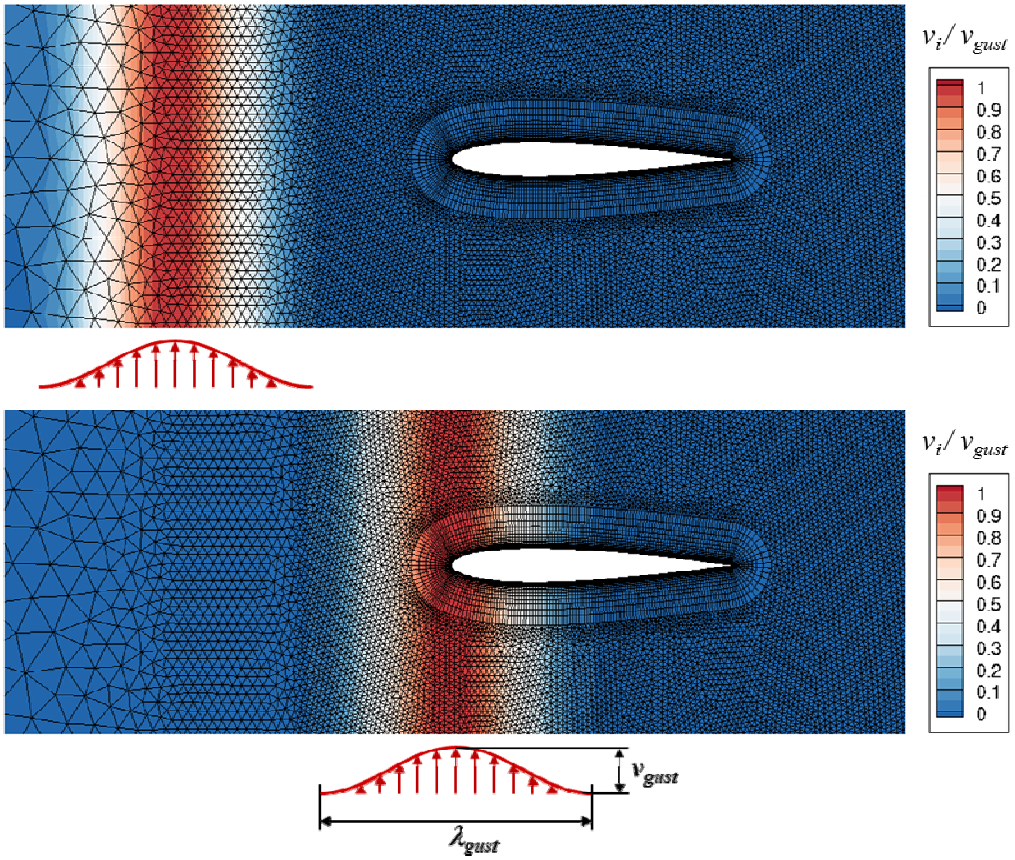

Figure 1: Disturbance velocity field traveling relative to an airfoil

To allow the simulation of wake vortex encounters, the model of Burnham and Hallock [6] has been implemented in TAU. The tangential velocity induced by a single vortex is described by

$$V_t = \frac{\Gamma}{2\pi} \frac{r}{r_c^2 + r^2} \cdot \tag{2}$$

Γ is the circulation of the vortex, r is the distance of a point in the flow field to the vortex axis and r_c is the vortex core radius. The disturbance velocity field of the wake vortices behind an aircraft can be modeled by superposition of two counter rotating vortices with distance b like sketched in Figure 2. Figure 3 shows the distribution of the tangential velocity induced by a pair of counter rotating Burnham-Hallock vortices in a plane through the vortex axis.

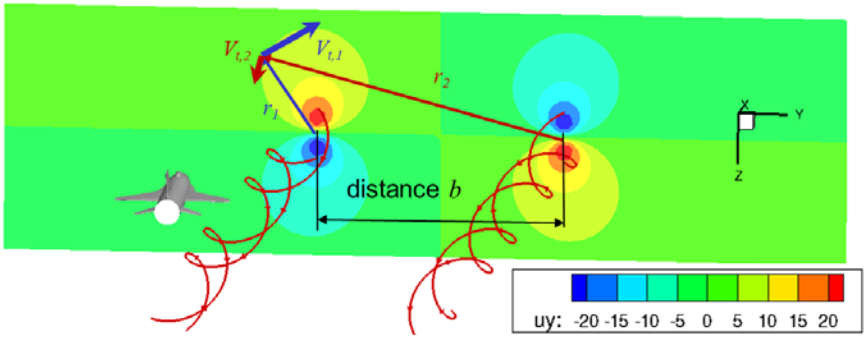

Figure 2: Disturbance velocity field (y-component) created by a pair of counter rotating vortices

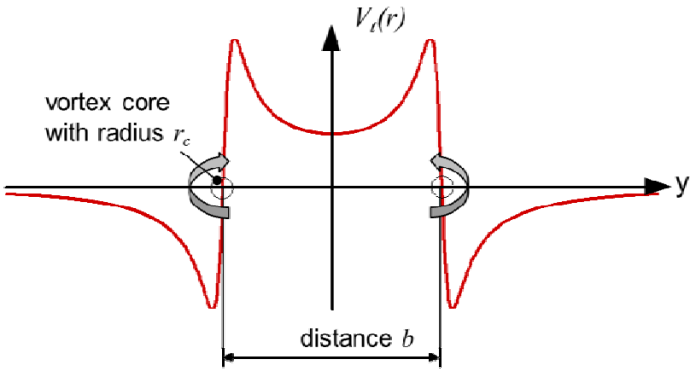

Figure 3: Distribution of tangential velocity induced by a pair of counter rotating Burnham-Hallock vortices in a plane through the vortex axis

2.2 Resolved Atmosphere Approach

To enable the simulation of a mutual interaction of aircraft and atmospheric disturbances like gusts and wake vortices, the resolution of the disturbances in the flow field is required. This can be realized by feeding them into the flow field at the far field boundary. Therefore, in TAU, the non-reflecting far field boundary condition based on the work of Whitfield [7] has to be adapted. For this boundary condition a far field state including velocity components u_{inf}, v_{inf}, w_{inf} has to be specified at the outer side of the discretized domain. Usually these values are constant at the whole far field boundary. For e.g. gust simulations the velocity components of the far field state can now be specified as a function of space and time.

2.3 Comparison of Resolved Atmosphere Approach and Disturbance Velocity Approach

2.3.1 Comparison for gusts

As already mentioned a disadvantage of the RAA is the requirement of high spatial resolution to transport atmospheric disturbances like gusts without too much numerical losses, since TAU is only of 2nd order accuracy in space. To minimize the effort necessary to transport a gust through the discretized flow domain from inflow boundary to the aircraft, a technique making use of “gust-transport-meshes” has been developed. The idea behind will be described for a simple 2D test case, which has been set up to compare the DVA and the RAA approach, see also [8]: The interaction of a symmetrical NACA0012 airfoil with a Horizontal Tail Plane (HTP) with a vertical gust. The grid used in this example is an overset mesh, as shown in Figure 4. An unstructured mesh containing wing and HTP (blue) are placed into a Cartesian background mesh (red). The distance between inflow boundary and wing is 20 chord lengths. A higher resolution normal to the wing plane is used close to the airfoils (up to a distance of z = ±3 chord lengths). The spacing is increased with growing distance from the airfoil and HTP, in order to safe mesh nodes. An additional grid (green) with a high resolution in flow direction is used for the “transport” of the gust from the far field boundary to the wing-HTP configuration. For time $t = 0s$, the gust is just in front of the computational domain. For time $t > 0s$, the gust is fed into the flow field at the left and the lower far field boundary marked blue in Figure 4. The position of the gust transport grid is unchanged, until the gust is centered in the gust transport mesh. Afterwards the grid is starting to move with the convection velocity u_{inf} of the flow.

To find an appropriate resolution of the gust transport mesh, a grid density study has been carried out in [8], using only the background grid and the gust transport grid. We assumed a short gust wavelength of only one grid unit, corresponding to the reference chord length of the wing (cases with longer wavelength are less critical). As gust amplitude 10% of the

convection speed is selected. Three different resolutions in flow direction have been tested: 25, 50 and 100 cells to resolve one gust wavelength. The outcome of the study has been that 100 grid cells are sufficient to transport the gust without significant numerical losses.

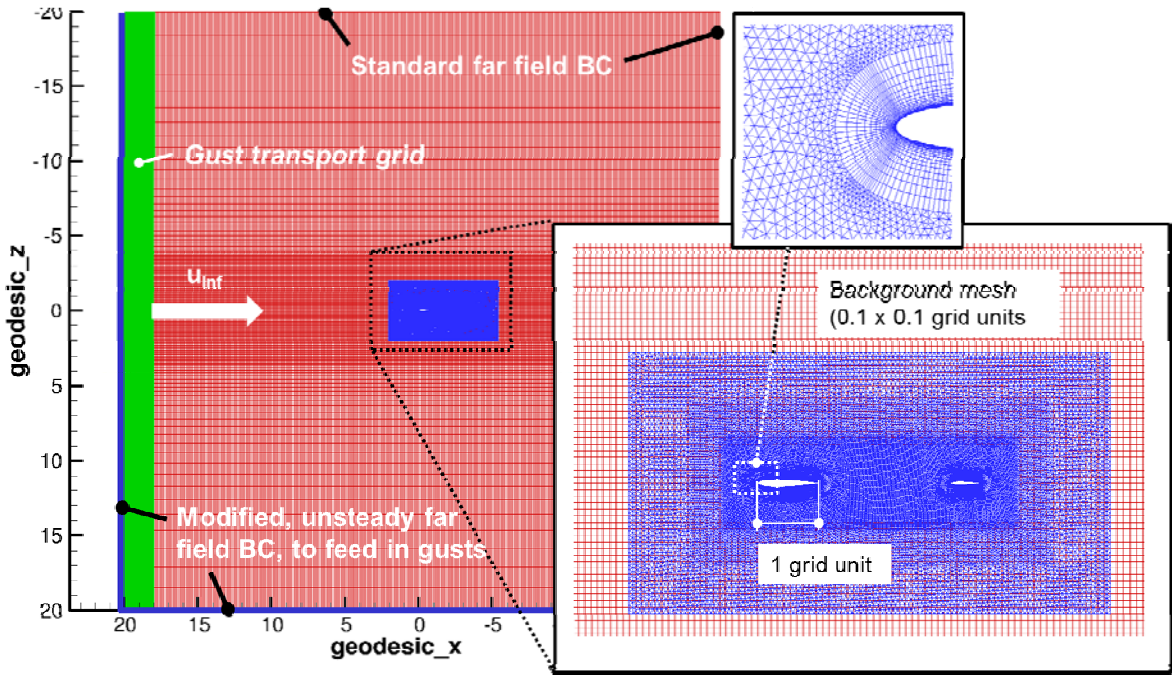

Figure 4: Overset grid setup for simulation of interaction of wing-HTP configuration with a gust of wavelength 1 grid unit (plotted in inertial (geodesic) coordinate system)

In previous work [8] a detailed analysis of gust encounter simulations restricted to two dimensional flow problems has been made using the grid shown in Figure 4. Computations have been made for 3 different gust wavelengths (1, 2 and 4 wing chord lengths). The classical "1-cos" gust shape has been used in the study. Two different on-flow Mach numbers have been used, to allow checking the influence of compressibility. Inviscid as well as viscous computations have been made. As measure for the prediction error of the DVA relative to the RAA, the maximum lift found during the simulation has been used:

$$err_{C_{L,\max}} = \frac{\left|C_{L,\max,RAA} - C_{L,\max,DVA}\right|}{\left|C_{L,\max,RAA}\right|} \tag{3}$$

The main outcome of the study has been that the DVA shows comparable results down to gust wave length of 2 chord lengths. The error in maximum lift has been below 3%, which is acceptable.

In this work we want to enhance the study towards three dimensional applications of realistic aircraft configurations, to check if the fuselage, which is long relative to c_{ref}, has a negative influence on the achieved global loads. We selected the so called LamAIR configuration [9] for our study, a configuration with forward swept wing and similar design mission like Airbus A320. The meshing philosophy used is the same, like in the 2D example. Figure 5 gives an impression of the mesh, containing 20×10^6 grid nodes. From an existing hybrid mesh of the configuration (Figure 5 left), a near field mesh has been extracted (Figure 5 middle) and embedded into a Cartesian background mesh (Figure 5 right). Simulations have been made again for 3 gust wave lengths with $\lambda / c_{ref} = 1, 2$ and 4. The Mach number is $Ma_\infty = 0.78$ in a flight altitude of 11 km. The gust amplitude is 10% of the undisturbed flow velocity. For all

simulations for the 3 wave lengths the lift versus time is plotted (Figure 6), the dashed line is associated to the DVA and the solid line is associated to the RAA. The prediction error of the DVA relative to the RAA according to equation 5 is summarized in Table 2. The trends are again the same, like in 2D. For the present 3D case even the shortest wave length shows a fair agreement between both approaches.

λ / c_{ref}	$err_{CL,max}$
1	1.42%
2	1.28%
4	0.42%

Table 1: Maximum lift prediction error of DVA relative to RAA (3D case)

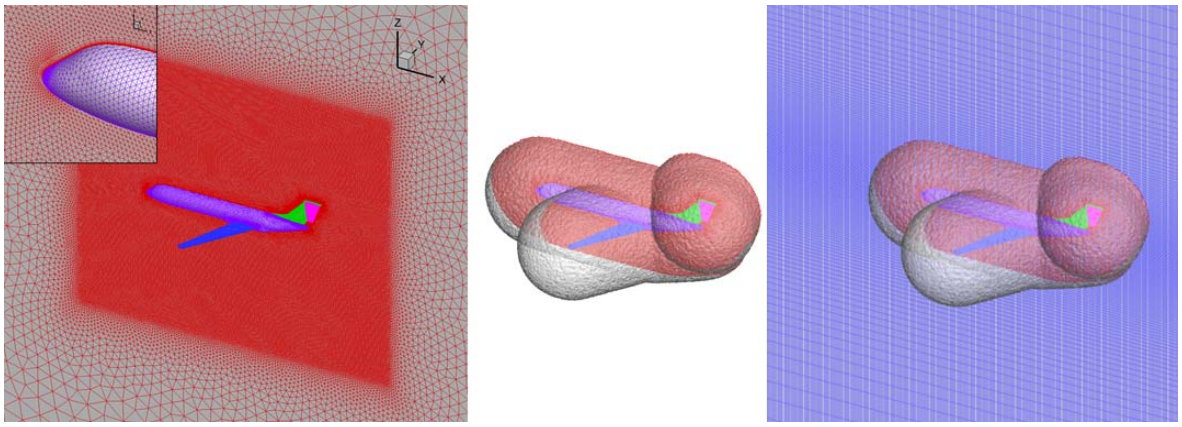

Figure 5: Overset grid setup for the simulation of 3D gust aircraft interaction

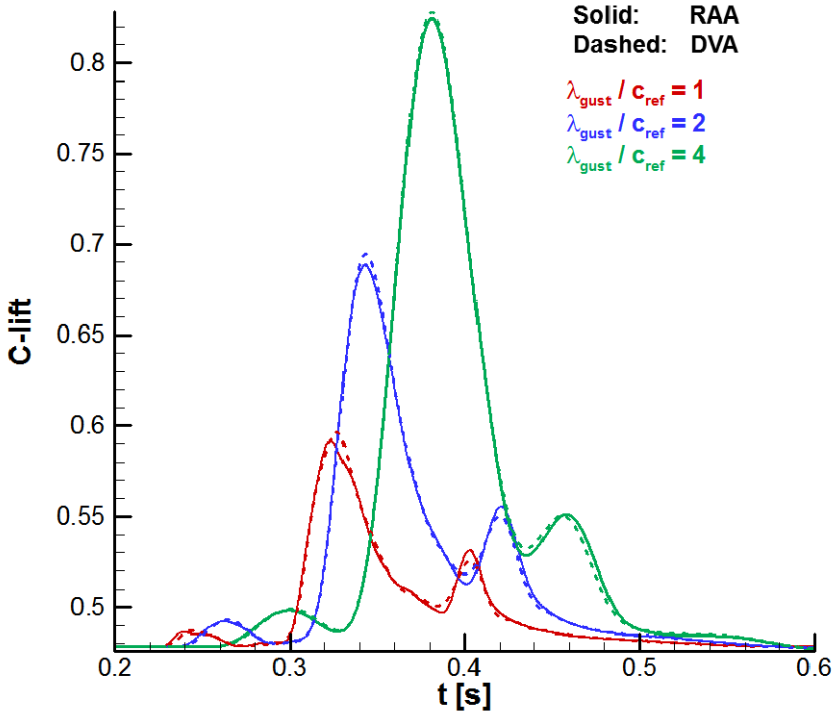

Figure 6: Comparison of lift versus dimensionless time predicted by DVA (dashed lines) and RAA approach (solid lines) for viscous flow

2.3.2 Comparison for wake vortices

A similar study like for gusts has also been made for wake vortices. A wing configuration with the span similar to an A320 is interacting with an isolated vortex of an A340. The circulation Γ is $486m^2/s$, the vortex core radius r_c is $2.4\ m$, the Mach number is set to 0.78, the angle of attack α is $0.0°$. We assume that the vortex axis is aligned with the flight direction of the wing. As wing geometry the so called LANN wing has been used [10]. An existing mesh for the half configuration has been doubled by mirroring. After scaling the mesh, to get a span similar to an A320, a nearfield grid has been created by removing all cells with a wall distance larger than a half root chord length. The nearfield grid (4.8 x 10^6 nodes) has been embedded into a Cartesian mesh with a high resolution in the area of the wing and the vortex (2.8 x 10^6 nodes), see Figure 7. The distance of the inflow boundary to the wing is approximately 3 half spans ($3s = 48m$).

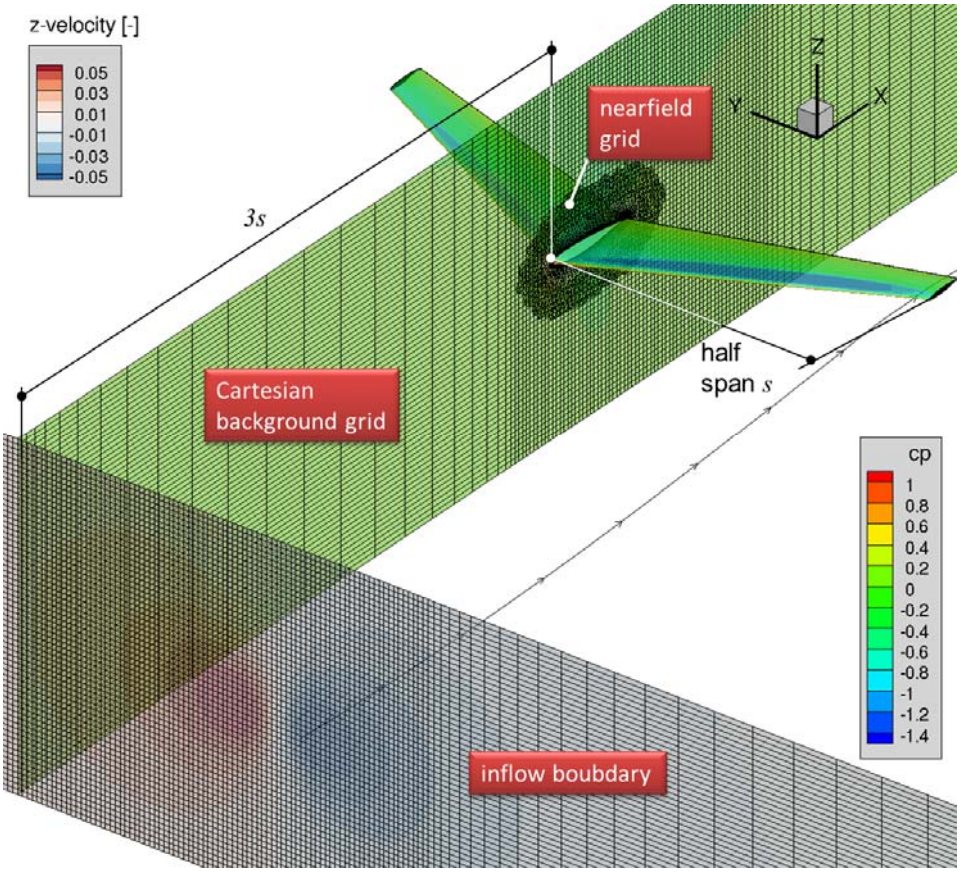

Figure 7: Grid setup for the simulation of a vortex encounter of the LANN wing

To find an adequate resolution of the mesh to resolve the vortex properly, a grid convergence study has been made in advance. A Cartesian mesh family has been generated, based on the finest mesh, see Figure 8. The distance of the in- and outflow boundary is the same as the distance from inflow boundary and leading edge of the wing ($3s$). The resolution of the mesh should be adjusted such, that the vortex is transported from in- to the outflow boundary without too large numerical losses. In the area of the vortex core 10 cells are used to resolve one vortex core radius in the finest grid, 5 cells on the medium and 2.5 cells on the coarsest grid. Figure 9 shows lines of constant velocity component w in z-direction on the inflow boundary (red) and the outflow boundary (dashed blue) for all grids. Even for the coarsest mesh the agreement is well, accept close to the vortex core. Figure 10 shows the distribution of the velocity component w for $z = 0$ (through the vortex core) versus the spanwise direction

y. The prescribed velocity distribution on the inflow boundary is plotted in red, the blue symbols belong to the computed velocity at the outflow boundary. Deviations are only visible on the coarsest mesh close to the vortex core. Following table gives an overview of the maximum error $err_{\max}$ and the average error err_{mean} for all three meshes. For the computation of the error all nodes on the mesh line $z = 0$ on the inflow boundary and outflow boundary are taken into account. The prescribed velocity components on the inflow boundary deal as reference. The errors are computed as

$$err_{\max} = \max\left(\frac{|w_{out,i} - w_{in,i}|}{w_{in,\max}}\right) * 100\% \quad \text{and} \tag{4}$$

$$err_{mean} = \frac{1}{N}\sum_{i=1}^{N}\left(\frac{|w_{out,i} - w_{in,i}|}{w_{in,\max}}\right) * 100\% \ . \tag{5}$$

	Fine mesh	Medium mesh	Coarse mesh
$err_{\max}$	0.90%	4.95%	15.88%
err_{mean}	0.11%	0.64%	2.57%

Table 2: Maximum and average error for the predicted *w*-velocity component

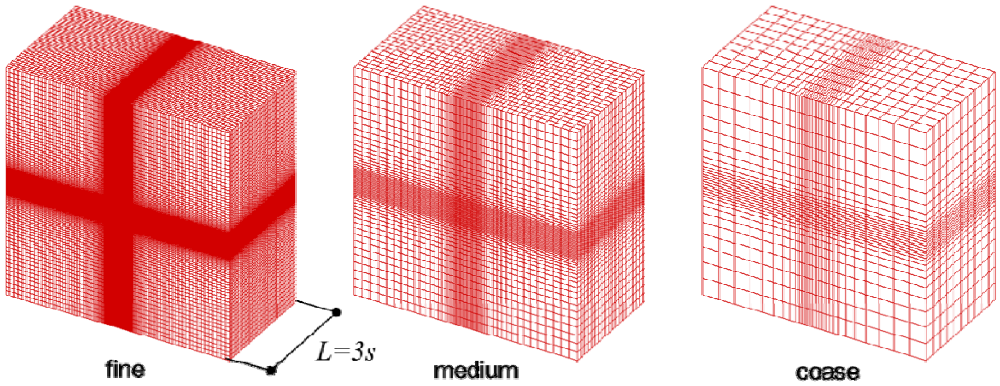

Figure 8: Grids for mesh resolution study; $s = 16m$ is the half span of the scaled LANN wing

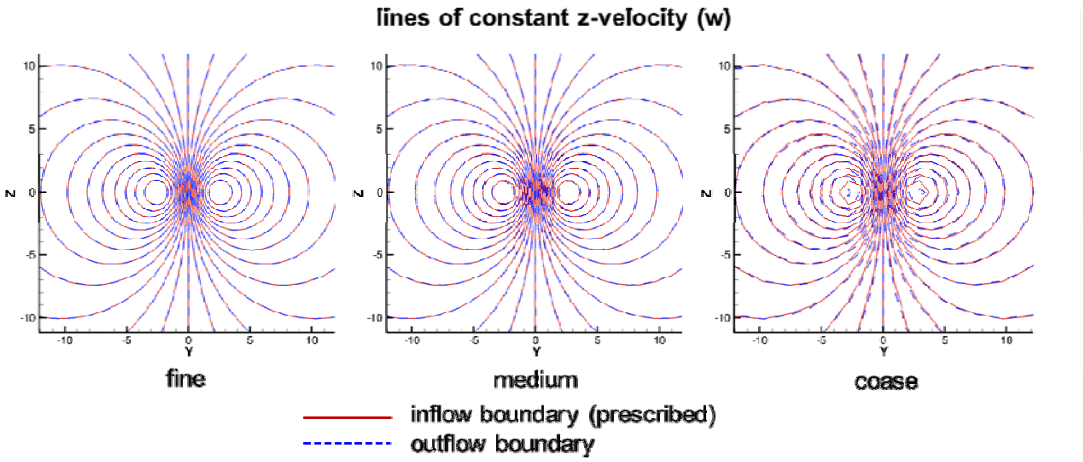

Figure 9: Lines of constant *z*-velocity (*w*) at in- and outflow boundary for the three different grid resolutions

If the user of a CFD code is primarily interested in global coefficients, the average error err_{mean} is of relevance. Since the mean error is below one percent for the medium and the fine

mesh, the resolution of both meshes should be sufficient for wake vortex encounter simulations using the RAA. To be on the safe side the fine resolution has been chosen for the background grid shown in Figure 7.

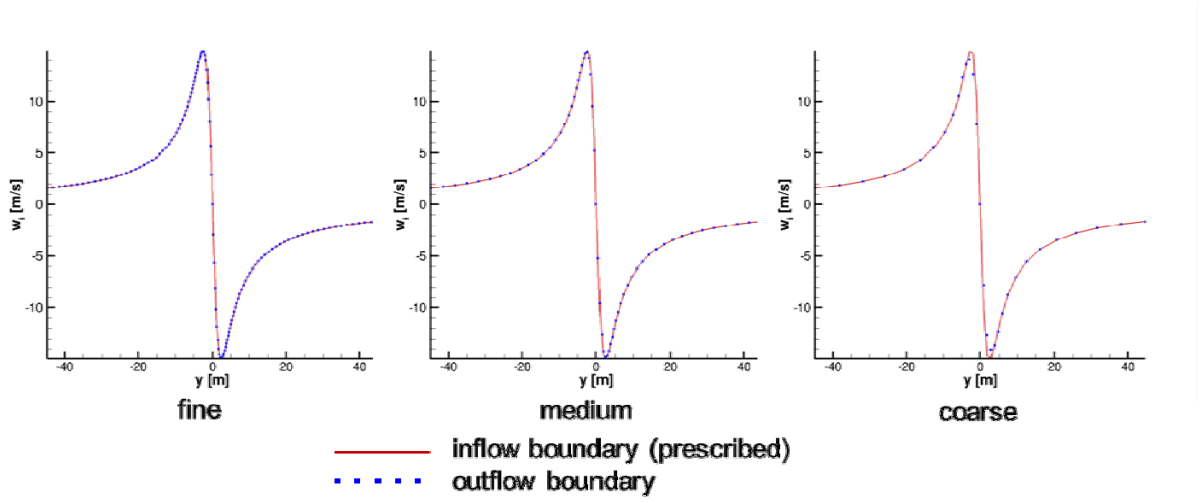

Figure 10: Distribution of *z*-velocity (w) for $z = 0$ at in- and outflow boundary for the three different grid resolutions

Using the mesh shown in Figure 7 the DVA and RAA have been compared in case a of vortex encounter. As already mentioned before, the wing, scaled to the size of an A320, interacts with an isolated vortex of an A340. The direction of the vortex axis is aligned with the flow direction. The position of the vortex axis is varied from the left to the right wing tip in steps of *2 m*. In total 34 steady simulations have been performed, 17 using the RAA and 17 using the simplified method, the DVA. Results for the resulting lift and rolling moment coefficient versus the spanwise position of the vortex are plotted for both methods in Figure 11. The lines belong to the results achieved with the DVA and the symbols to the RAA predictions. The agreement of the predictions of the DVA and RAA is excellent.

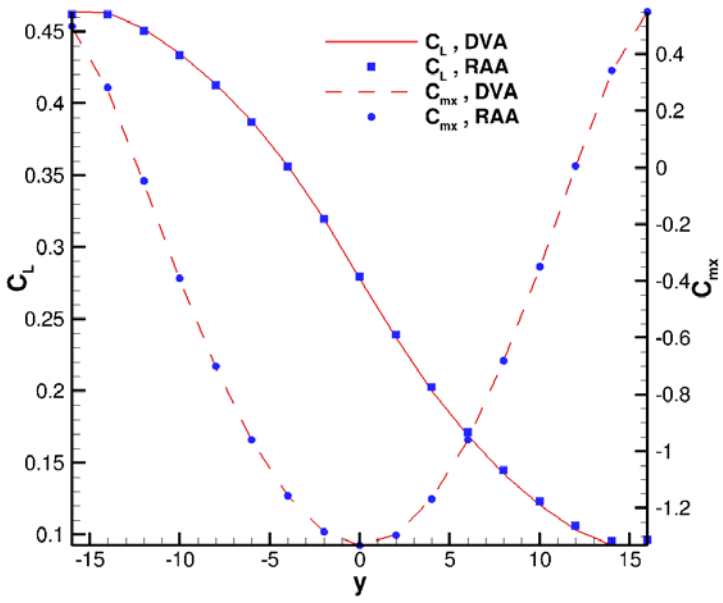

Figure 11: Comparison of results of lift and rolling moment coefficient using the DVA and RAA

The relative prediction error of the DVA relative to the RAA is plotted for the lift and rolling moment coefficients in Figure 12. The error is defined as

$$err_{CL,i} = \left| \frac{C_{L,i,DVA} - C_{L,i,RAA}}{C_{L,\max,RAA} - C_{L,\min,RAA}} \right| * 100\% , \tag{6}$$

with i being the position index of the vortex axis ($1 \leq i \leq 17$). For all positions the error is below *1%*. So we can conclude that the simple DVA is an appropriate method for wake vortex encounter simulations. Such an application is presented in next chapter.

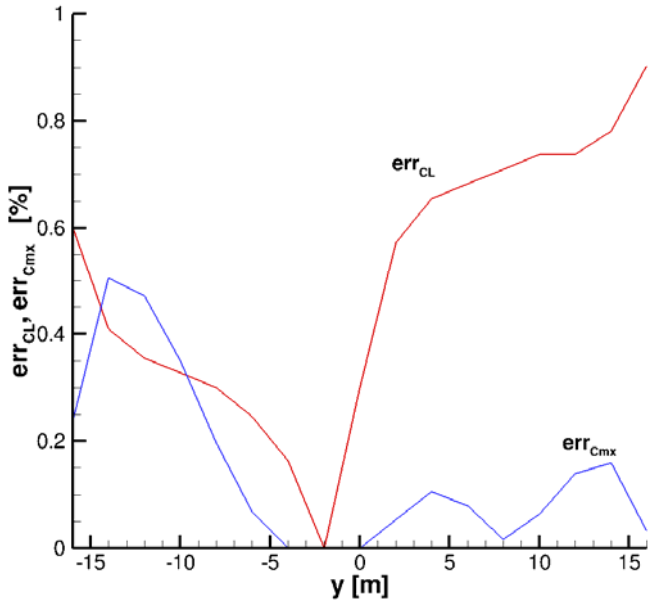

Figure 12 Prediction error of DVA relative to the RAA for the lift and the rolling moment coefficient

3 APPLICATION: COUPLED SIMULATION OF A WAKE VORTEX ENCOUNTER

To demonstrate the simulation of a wake vortex encounter, as geometry the so-called SDM configuration [11] has been selected, which is a generic fighter configuration similar to an F16. We assume the aircraft is set to fly horizontally close to sea level with a Mach number of $Ma_{inf} = 0.5$. The aircraft encounters a wake vortex of an aircraft in front with approximately double weight of the SDM configuration ($m_{SDM} = 9t$, $m_{leading\ aircraft} = 20t$). The circulation of the vortices is $\Gamma = 158m^2/s$, the vortex core radius is $r_c = 1m$ and the distance of the axis of the pair of vortices is $b = 21.5m$. To take into account the reaction of the aircraft, TAU is coupled to a six degrees of freedom flight mechanics module. For details of the coupling procedure and the flight mechanics module, the reader is referred to [12].
Figure 13 left shows the initial situation. The right wing tip of the horizontally flying aircraft is *20m* above the left vortex core. At $t = 0s$ the pilot decides to reduce the flight level. Therefore he deflects the HTP, which is also acting as elevator, for *1s*. The time history of the HTP (Horizontal Tail Plane) is plotted in red in Figure 13, right. With the reduction of the flight level, the influence of the clockwise rotating vortex increases. The effect of the vortex is an upwind at the outer wing. This results in an anticlockwise rolling moment and the aircraft starts to roll, see Figure 14. To compensate the rolling moment and to roll pack the pilot makes use of the ailerons. The corresponding deflection history is plotted in blue in Figure 13 - Figure 15. The actual deflection angle fitting to the aircraft position in these figures is marked with a circle. The aircraft starts to roll back but still reduces the flight level. After *5s*

the pilot starts to pull up the aircraft, making use of the HTP again. This creates a nose up pitching moment. The angle of attack is increasing and therefore, after about 6s, the aircraft starts to climb again. Figure 16 shows the history of the flight level in geodesic coordinate z_{geo}. Please note that the z_{geo}-*axis* is pointing downward. Furthermore the history of the rolling angle Φ is plotted. Although the pilot reacts, the maximum rolling angle is about 50 degrees, which underlines the hazardousness of wake vortices especially for small aircrafts.

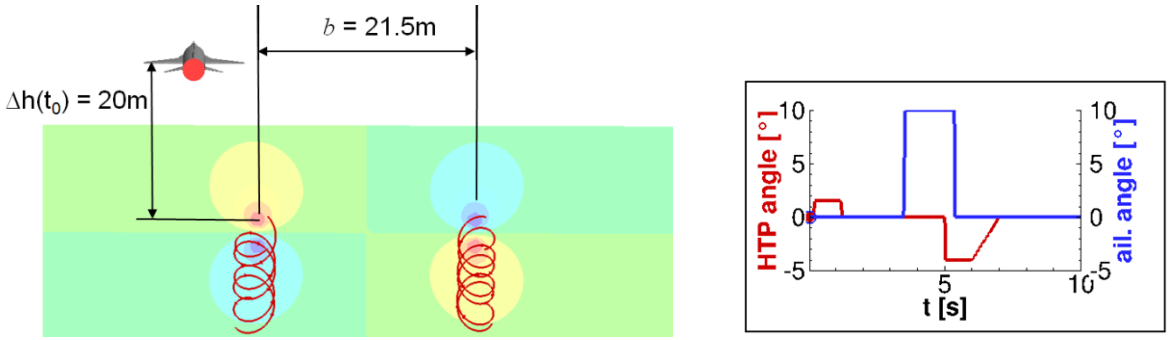

Figure 13: Left: Initial position of a generic fighter aircraft relative to wake vortices of leading aircraft for t = 0s; Right: History of elevator angle and aileron angle relative to the trimmed state

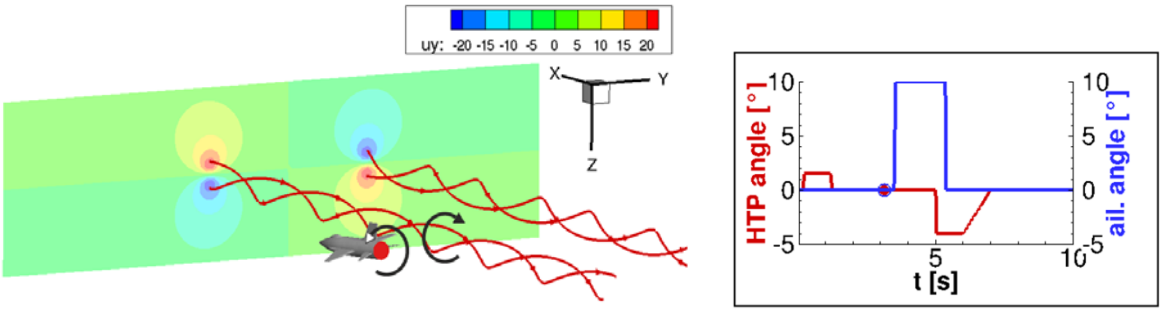

Figure 14: Position of the aircraft for t = 3s

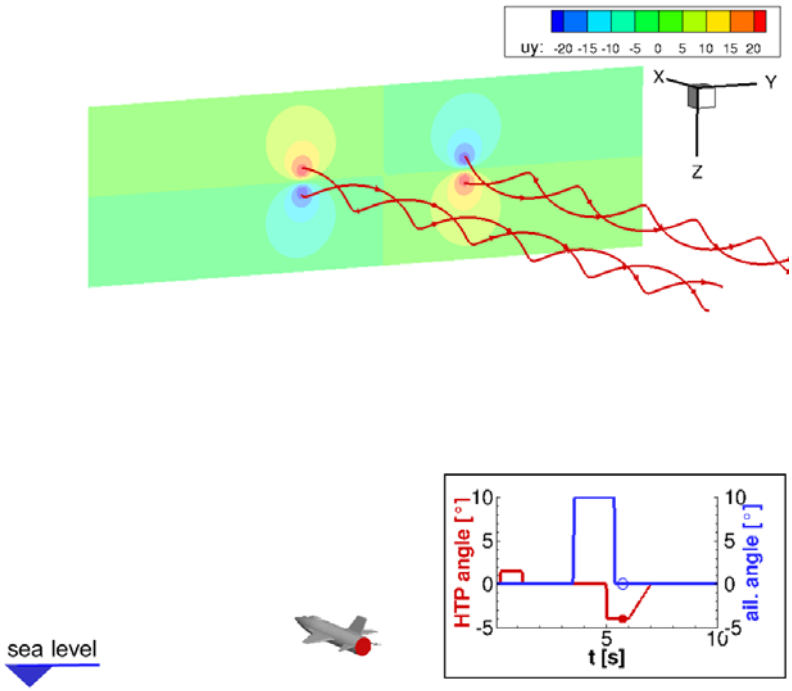

Figure 15: Position of the aircraft for t = 5.7s

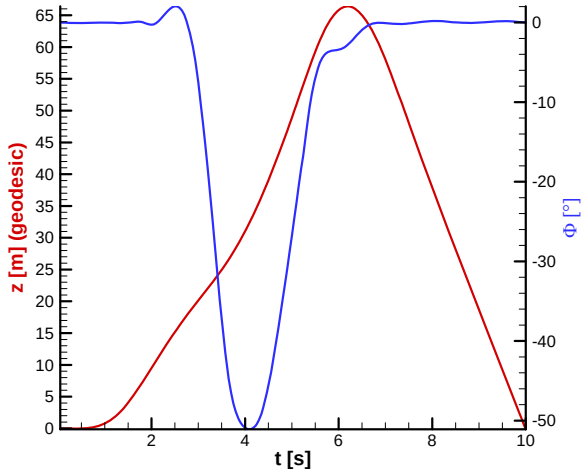

Figure 16: History of the aircraft's altitude (note: z-axis is pointing downward) and rolling angle Φ

4 SUMMARY AND CONCLUSIONS

Two different methods for modeling of gusts and wake vortices have been implemented into the CFD code TAU:

1. A simplified method called DVA allowing the usage of standard CFD meshes. The disadvantage is that the mutual interaction of gusts / wake-vortices and aircraft is not captured;
2. A method resolving atmospheric disturbances in the flow field, allowing the simulation of a mutual interaction of aircraft and disturbance (RAA). They are fed into the flow field via an unsteady boundary condition. The disadvantage is that a high mesh resolution is required to resolve the atmospheric phenomena properly.

Both methods have been compared in terms of global loads for gust and wake vortex encounter simulations in 3D. The results prove that the simplified method is well suited to predict global loads properly. In case of gusts, even for short dimensionless gust wavelengths $\underline{\lambda} = \lambda / c_{ref}$ down to a value of *1* reasonable results are achieved.
The applicability of the DVA for industrial configurations has been demonstrated for the simulation of the interaction of a generic fighter aircraft with the wake vortex of an aircraft with double weight.

5 REFERENCES

[1] Schwamborn, D., Gerhold, T., Heinrich, R.: The DLR TAU-Code: Recent Applications in Research and Industry. In Proceedings of "European Conference on Computational Fluid Dynamics" ECCOMAS CDF 2006, Egmond aan Zee, The Netherland, 2006.

[2] Heinrich, R.: Numerical Simulation of Wake-Vortex Encounters Using the Chimera-Technique. STAB-Symposium 2000 in Stuttgart, in New Results in Numerical and Experimental Fluid Mechanics III, Springer, 2002

[3] Sitaraman, J., Baeder, j. D.: Field Velocity Approach and Geometric Conservation Law for Unsteady Flow Simulations, AIAA JOURNAL, Vol. 44, No. 9, DOI: 10.2514/1.5836 September 2006

[4] Kroll, N., Fassbender, J. K. (eds): MEGAFLOW - Numerical Flow Simulation for Aircraft Design. Notes on Numerical Fluid Mechanics and Multidisciplinary Design (NNFM), 89, Springer-Verlag, 2005

[5] Heinrich, R., Michler, A.: Unsteady Simulation of the Encounter of a Transport Aircraft with a Generic Gust by CFD Flight Mechanics Coupling, CEAS Conference 2009, Manchester, 2009

[6] Burnham, D., C., Hallock, J., N. Chicago Monoacoustic: Vortex Sensing System Vol. 4, Wake Vortex Decay, Springfield, VA, National Information Service, 1982

[7] Whitfield, D. L., Three-dimensional unsteady Euler Equation solutions using flux vector splitting, NASA contractor report NASA CR-173254, 1983

[8] Heinrich, R., Reimer, L.: Comparison of Different Approaches For Gust Modelling in the CFD Code TAU, International Forum on Aeroelasticity & Structural Dynamics 2013, 24. - 27. Juni 2013, Bristol, Großbritannien, 2013

[9] Seitz, A., Kruse, M., Wunderlich, T., Bold, J., Heinrich, L.: The DLR Project LamAiR: Design of a NLF Forward Swept Wing for Short and Medium Range Transport Application. In: 29th AIAA Applied Aerodynamics Conference. AIAA Conference Paper AIAA 2011-3526. June 2011

[10] Zwaan, I. R. J.: LANN Wing Pitching Oscillations, Compendium of Unsteady Aerodynamic Measurements, AGARD-R-702 Addendum No. 1, Aug. 1982.

[11] Zan, S. et al: Wing and Fin Buffet on the Standard Dynamic Model, RTO Technical Report, RTO-TR-26, pp 361-381, 2000

[12] Reimer, L., Heinrich, R., Meuer, R.: Validation of a Time-Domain TAU-Flight Dynamics Coupling Based on Store Release Scenarios. In: New Results in Numerical and Experimental Fluid Mechanics IX Notes on Numerical Fluid Mechanics and Multidisciplinary Design 124, Springer Verlag. Seiten 455-463. ISBN 978-3-319-03157-6. ISSN 1612-2009, 2014

6 ACKNOWLEDGEMENT

The research leading to these results has partly been supported by the AEROGUST project funded by the European Commission under grant agreement number 636053 and the German research project FOR 1066 “Simulation des Überziehen von Tragflügeln und Triebwerksgondeln” funded by the “Deutsche Forschungsgemeinschaft DFG”.

7 COPYRIGHT STATEMENT